

Critical currents of superconducting microbridges*

W. J. Skocpol

Department of Physics, Harvard University, Cambridge, Massachusetts 02138

(Received 15 March 1976)

The critical currents of long uniform superconducting tin microbridges ranging in width from 0.3 to 10 μm have been measured. In the narrowest bridges the current density is nearly uniform and the magnitude and temperature dependence of the critical-current density agree with the Ginzburg-Landau prediction. In wider bridges the current density becomes peaked at the edges of the film and the magnitude and temperature dependence of the critical current are altered. Theoretical calculations of the nonlocal linear electrostatics together with adjustment of the nonlinear peak current density to include coherence-length effects appear adequate to explain both the magnitude and the temperature dependence of the critical currents in the wider bridges.

I. INTRODUCTION

It is generally accepted that the ultimate limit on the current-carrying capacity of superconductors is reached when further acceleration of the superconducting electron pairs would lead to such a rapid decrease of their number that the current-carrying capacity reaches a maximum. For spatially uniform current flow, this situation is easily described within the Ginzburg-Landau theory, and leads directly to the GL critical-current density,¹

$$J_c^{\text{GL}} = (c/3\sqrt{6}\pi) [H_c(T)/\lambda(T)], \quad (1)$$

where $H_c(T)$ is the thermodynamic critical field and $\lambda(T)$ is the penetration depth. In many experimental situations, however, the current density is not uniform, and the critical current observed in a thin-film conductor of width W and thickness d is less than $(Wd)J_c^{\text{GL}}$, often by a considerable factor. Nonuniform current flow can be caused either by the tendency of the current density to peak at the edges of a wide strip²⁻⁴ or by the entry of current vortices (flux lines) into the film.⁵

Early experimental studies of the critical currents of wide thin films proved difficult to interpret quantitatively because of the peaking of the current density at the edges.⁶ The most successful results were achieved by Glover and Coffey,⁷ who used an analytic approximation to the current distribution to extract a peak current density, which was similar in magnitude and temperature dependence to J_c^{GL} . Since then, Hunt⁸ and Andratskii *et al.*⁹ have studied the critical currents of much narrower thin-film microbridges. Hunt concluded that the uniform J_c^{GL} was achieved in bridges about 1- μm wide, but that critical currents of bridges wider than about 3 μm were smaller than expected, perhaps because of the entry of vortices. Andratskii *et al.* concluded that

the critical currents of geometrically uniform bridges about 2- μm wide could be explained by the use of an approximate expression for the peaking of the current density at the edges at low temperatures, where the penetration depth is small. They also showed that greatly reduced critical currents could result from the entry of vortices at pronounced edge defects.

In the course of other experiments,^{10,11} we have accumulated critical-current data for a number of long, geometrically uniform, well-characterized tin microbridges ranging in width from 0.3 to 10 μm . The bridges were cut from 0.1- μm films using a diamond knife, which gives uniform edges on the scale of 0.1 μm .¹¹ The data on the narrower ($\sim 1 \mu\text{m}$) bridges agree very precisely with the magnitude and temperature dependence of J_c^{GL} , but the wider bridges differ systematically in both the magnitude and temperature dependence of the critical current.

We have carefully examined the theoretical problem of computing the depairing critical current of the wider bridges taking into account the peaking of the current distribution at the edges, and we find that certain approximate solutions give a good account of the observed data. Our calculations consider both a rounding of the peak current density by the nonlocal electrodynamic response, and an enhancement of the maximum peak current density above J_c^{GL} when the coherence length $\xi(T)$ exceeds the penetration depth $\lambda(T)$.

II. EXPERIMENTAL DATA

In order to compare our experimental critical currents with the values expected for uniform current flow at the GL critical-current density, we have plotted the scaled quantity $I_c(T)/I_c(0)$, where

$$I_c(0) = (Wd)cH_c(0)/3\sqrt{6}\pi\lambda_{\text{eff}}(0). \quad (2)$$

TABLE I. Sample parameters.

Sample	a	L (μm)	W (μm)	d (μm)	l (μm)	$I_c(0)$ (mA)
33	\triangle	3.0	1.0	0.10	0.06	19
35	\circ	3.0	1.0	0.11	0.08	23
36	\square	2.0	0.7	0.066	0.10	11
37	\blacktriangle	30	0.4	0.066	0.18	7.0
38	\blacksquare	30	0.35	0.066	0.19	6.3
45	+	37	1.0	0.11	0.063	21
47	\bullet	50	1.3	0.10	0.07	26
50	\square	42	3.0	0.11	0.06	62
51	\circ	19	3.0	0.11	0.07	66
39a	\blacktriangle	65	8.0	0.066	0.12	126
39b	+	65	7.0	0.066	0.12	110
41	\blacksquare	75	7.5	0.13	0.06	184
42	\blacktriangle	75	7.5	0.13	0.06	184
43	\bullet	40	8.0	0.10	0.06	151

^a These symbols are those used in Figs. 1 and 2, respectively.

The width W of each bridge (as well as its length) was observed directly using a scanning electron microscope, and the thickness d was determined by a quartz-oscillator deposition monitor calibrated by use of an optical interferometer. The effective penetration depth can be written $\lambda_{\text{eff}}(T) = [1 + \xi_0/J(0, T)l]^{1/2}\lambda_L(T)$, which gives a close approximation to the correct mean-free-path dependence due to nonlocal electrodynamics.¹² Since $J(0, T)$, which is the BCS kernel for the nonlocal relation between \vec{J} and \vec{A} evaluated at $\vec{R}=0$, is only weakly temperature dependent, varying from 1 at $T=0$ to 1.33 at $T=T_c$, we shall ignore this temperature dependence and take $J(0, T)=1.2$. The mean free path l is determined from the observed dimensions and the normal resistivity above T_c using $\rho l = 10^{-11} \Omega \text{ cm}^2$. The other necessary material parameters for tin are $H_c(0) = 306 \text{ Oe}$, $\xi_0 = 2300 \text{ \AA}$, and $\lambda_L(0) = 350 \text{ \AA}$. Table I gives the relevant parameters for all samples for which data will be reported in this paper.

If the GL theoretical prediction Eq. (1) is scaled in this manner, the result is a sample-independent function

$$F(T) = \frac{I_c(T)}{I_c(0)} = \frac{H_c(T)}{H_c(0)} \frac{\lambda_L(0)}{\lambda_L(T)}, \quad (3)$$

where we will use the function $H_c(T)/H_c(0)$ measured for tin,¹³ and the function $\lambda_L(T)/\lambda_L(0)$ computed from microscopic theory.¹⁴ From the more approximate temperature dependences $H_c(T) \propto (1-t^2)$ and $\lambda(T) \propto (1-t^4)^{-1/2}$, we see that the temperature dependence of I_c is approximately $(1-t^2)^{3/2}(1+t^2)^{1/2}$, which reduces to the familiar $(1-t)^{3/2}$ mean-field dependence near T_c .

In Fig. 1, we show data for a number of long tin

microbridges, all approximately $0.1\text{-}\mu\text{m}$ thick and approximately $1 \mu\text{m}$ or less wide, scaled in the manner described above, as a function of the reduced temperature $t = T/T_c$. (T_c for these films is approximately 3.85 K , varying by 1% or 2% from sample to sample.) There are no adjustable parameters. The dashed curve which runs through the middle of the data is the function $F(T)$ defined in Eq. (3). The agreement between theory and experiment is excellent, with the values of $I_c(0)$ determined above scaling the data to agree with $F(T)$ to within 10%.

In Fig. 2, we show data scaled in the same manner for a number of microbridges of varying widths from 3 to $10 \mu\text{m}$. Here we see systematic, substantial departures from the GL result. These departures increase in the wider bridges. The temperature dependence of the data for each bridge is approximately $1-t^2$, except very near to T_c , as may be seen by comparison with the shape of the dotted curve. These are the data which we will show are explained by nonuniform current flow across the width of the bridge.

III. THEORETICAL APPROACHES

To see the importance of nonuniform current density, we turn to an approximation to the actual current distribution, suggested by Bowers.¹⁵ In the interior of a wide film, the current is approximated by

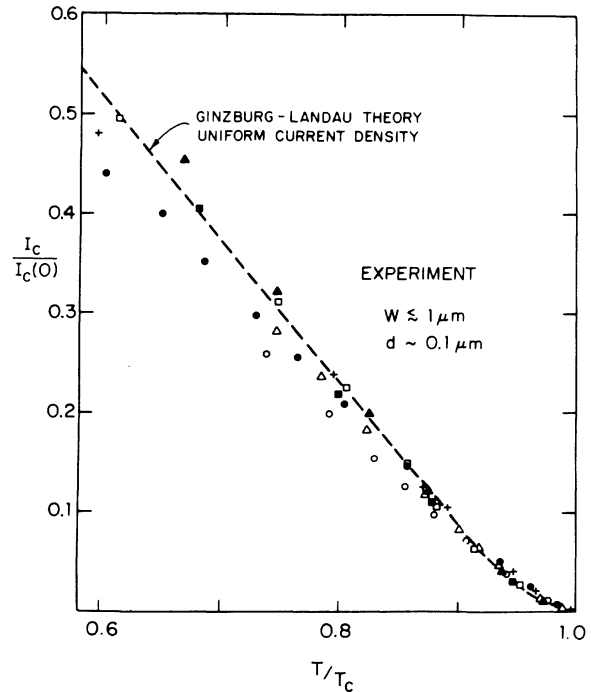


FIG. 1. Scaled critical currents of narrow tin microbridges showing agreement with simple GL theory.

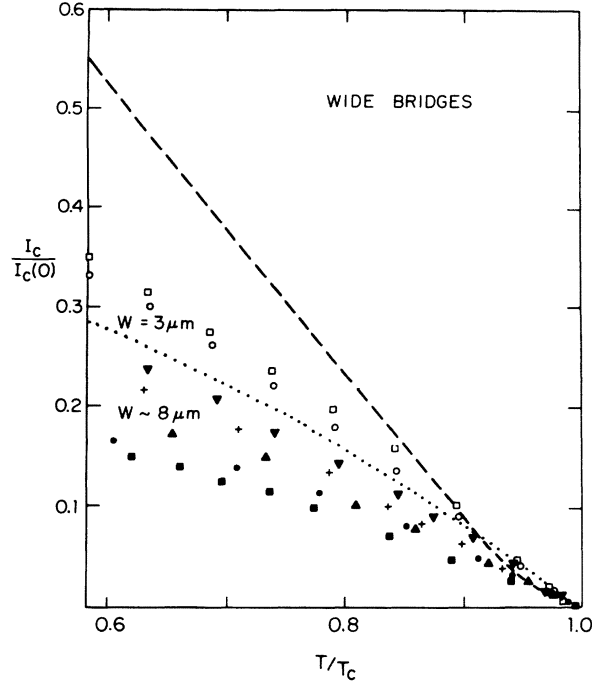


FIG. 2. Scaled critical currents of wider tin microbridges showing systematic departures from simple GL theory (dashed curve). The dotted curve illustrates the shape of a $1-t^2$ dependence, which gives better agreement.

$$J(x) = J(0)[1 - (2x/W)^2]^{-1/2}, \quad (4)$$

while near the edges it is approximated by

$$J(x) = (eW/2\lambda_{\perp})^{1/2} J(0) \exp[(x - \frac{1}{2}W)/\lambda_{\perp}], \quad (5)$$

where $\lambda_{\perp} = b\lambda_{\text{eff}}^2(T)/d$, $e = \exp(1)$, and b is a constant of order unity. The choice $b=2$ is common.^{4,16}

For $W \gg \lambda_{\perp}$, the two forms match in value and slope at a distance $\frac{1}{2}\lambda_{\perp}$ from edge of the film. The total current carried through the bridge is given by $I = \frac{1}{2}\pi W d J(0)$, and the maximum current density reached is $J(\frac{1}{2}W)$. If we assume that the critical current occurs when $J(\frac{1}{2}W)$ reaches J_c^{GL} , then

$$\frac{I_c(T)}{I_c(0)} = \pi \left[\frac{\lambda_{\perp}(0)}{2eW} \right]^{1/2} \frac{H_c(T)}{H_c(0)}, \quad (6)$$

where $I_c(0)$ is defined in Eq. (2). The temperature dependence of H_c is approximately $1-t^2$ like that observed in the data from wide bridges. However, for $b \sim 1$, the coefficient in Eq. (6) is approximately a factor of 4 smaller than that observed in the data. This suggests that the current distribution is too sharply peaked at the edges, in this approximation.

To solve the general theoretical problem exactly within the Ginzburg-Landau theory requires the simultaneous and self-consistent solution of two

coupled nonlinear second-order partial-differential equations: one for the spatial variation of the magnitude of the order parameter and the other for the spatial variation of the vector potential, where within the superconductor the vector potential is directly related to the pair momentum. It is necessary also to consider the variations of the vector potential outside of the superconductor, so that the current distribution and corresponding magnetic fields are self-consistent. This formulation in terms of nonlinear partial-differential equations is very difficult to solve. In particular, even for simple geometrical representations of wide bridges, the two-dimensional problem does not reduce to a simple one-dimensional one because the transverse and external variations of the vector potential contain essential information about the magnetic field.

Therefore, the standard approach is to separate the problem of determining the current distribution using linear electrostatics from the problem of determining the nonlinear limits in the region of peak current density. Within this approach, we have extended previous work by examining (i) the effects of nonlocal electrostatics on the current distribution, and (ii) a related one-dimensional nonlinear problem to test whether it is accurate to equate the peak current density with J_c^{GL} to determine the critical current.

IV. NONLOCAL ELECTRODYNAMICS

As has been previously noted,^{2-4,17} the easiest way to formulate the linear electrostatics is in terms of integral equations. The integral relation between the vector potential \vec{A} and the current density \vec{J} derived from Maxwell's equations is given by

$$\vec{A}(\vec{r}) = \vec{\nabla}\phi + \frac{4\pi}{c} \int \frac{\vec{J}(\vec{r}')}{|\vec{r} - \vec{r}'|} d^3r', \quad (7)$$

where ϕ is an arbitrary scalar function. In the absence of an externally applied magnetic field and with the gauge choice $\text{div } \vec{A} = 0$, the term $\vec{\nabla}\phi$ is reduced to a constant C_0 .

In the geometry of our bridge, shown in Fig. 3, \vec{J} and \vec{A} take the form $J(x, y)\hat{z}$ and $A(x, y)\hat{z}$, and are symmetrical about $x=0$. Equation (7) then takes the form

$$A(x, y) = C_0 - \frac{2}{c} \int J(r') \ln|r - r'| dx' dy'. \quad (8)$$

Since our bridge is thin in the \hat{y} direction, we can assume that the current is uniform across the thickness of the bridge, and can perform the y' integration explicitly for $y=0$. Finally, if we consider a symmetrical grid of $2N+1$ points $x_{\pm i}$, $i=0, N$, with the associated values $J(x_{\pm i}, 0) = J_i$

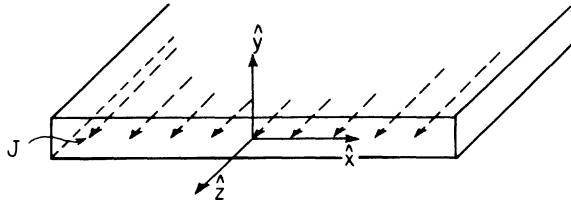


FIG. 3. Geometry of nonuniform current flow in a microbridge of rectangular cross section.

and $A(x_{\pm i}, 0) = A_i$, the integral equation (8) can be approximated by a set of $N+1$ linear equations of the form

$$A_i + \sum_{j=0}^N J_j G_{ij} \Delta x_j = C_0, \quad i = 0, N \quad (9)$$

where the contributions from both symmetrically disposed intervals are included in G_{ij} . Here Δx_j is the length of the interval around x_j .

At this point one could assume the London relation

$$\vec{J}(\vec{r}) = -(c/4\pi\lambda^2) \vec{A}(\vec{r}) \quad (10)$$

to reduce Eq. (9) to $N+1$ unknowns, and then solve the set of equations directly to obtain the current distribution J_i . The constant C_0 serves as a normalization constant which allows the integral of the current density to be adjusted to the total transport current I . Such a calculation has been carried out by Marcus,³ and Likharev.⁴ The current distribution peaks up at the edges, as expected.

The relation assumed in Eq. (10) is strictly local, in that \vec{J} is proportional to \vec{A} at that point, not to an integral over values in the neighborhood. Since the critical current depends sensitively on the maximum value of a sharply peaked current distribution, such averaging could affect the result.

To incorporate nonlocality explicitly, we have assumed a nonlocal relation between \vec{J} and \vec{A} of the Chambers-Pippard form:

$$\vec{J}(\vec{r}) = -\frac{3c}{(4\pi)^2 \xi_0 \lambda_L^2} \int \frac{\vec{R}[\vec{R} \cdot \vec{A}(\vec{r}')] }{R^4} e^{-R/\xi} d^3r', \quad (11)$$

where $R = |\vec{r} - \vec{r}'|$ and $\xi^{-1} = \xi_0^{-1} + (\alpha l)^{-1}$ with α a constant of order unity. We again assume that \vec{J} and \vec{A} do not vary in the \hat{y} and \hat{z} directions, and again direct our attention to the values J_i and A_i at the set of points $(x_{\pm i}, 0)$. The y' and z' integrations are carried out numerically. The integral equation (11) can then be approximated by a set of $N+1$ equations of the form

$$J_i + \sum_{j=0}^N A_j K_{ij} \Delta x_j = 0, \quad i = 0, N \quad (12)$$

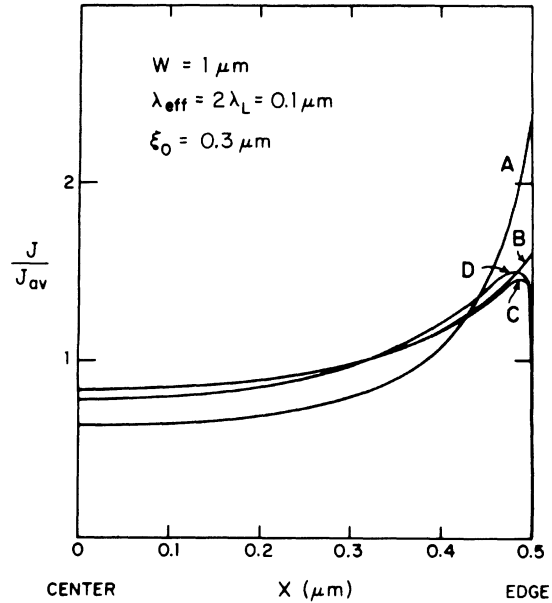


FIG. 4. Theoretical current distributions. Curve A: Bowers analytic approximation. Curve B: "Local" solution with $\lambda = \lambda_{\text{eff}}$. Curve C: "Pseudolocal" solution with small ξ_0 and $\lambda = \lambda_{\text{eff}}$. Curve D: "Nonlocal" solution with real ξ_0 and λ_L .

similar to (9). Then the $2N+2$ equations in $2N+2$ unknowns J_i and A_i contained in Eqs. (9) and (12) can be solved. Again C_0 serves to normalize J to correspond to the total transport current.

One of the well-known effects of nonlocal electrodynamics is to introduce the mean-free-path dependence of the penetration depth. Thus Eq. (9) starts explicitly with the London penetration depth $\lambda_L(0)$, but the calculated distributions fall off with the characteristic length λ_{eff} . Thus the use of λ_{eff} in any local approximation already includes much of the effect of nonlocality.

In Figs. 4 and 5, we show the current distributions calculated from these various theories, normalized so that the total current carried in each

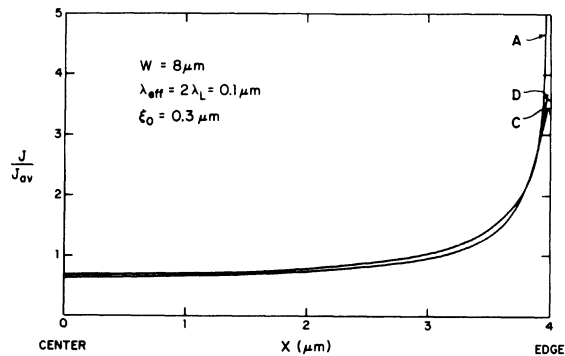


FIG. 5. Theoretical current distributions for a wider bridge. The curves are identified as in Fig. 4.

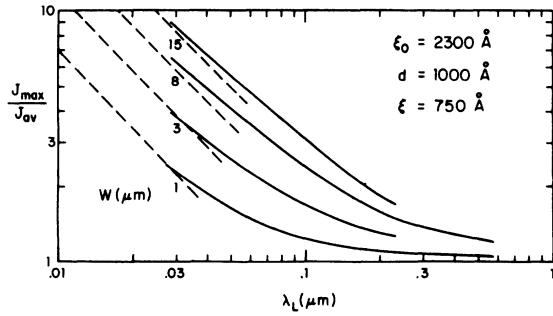


FIG. 6. Peak current density as a function of λ_L for various widths. The solid curves are the nonlocal theory and the dashed curves are the Bowers approximation, taking the parameter $b = 4$ for best agreement.

case is the same. We have used the values $\xi_0 = 3000 \text{ \AA}$, $\alpha l = d = 1000 \text{ \AA}$, and $J(0, T) = 1$, so that $\lambda_{\text{eff}} = 2\lambda_L$.

Figure 4 is for a bridge $1\text{-}\mu\text{m}$ wide with $d = \lambda_{\text{eff}} = 0.1 \mu\text{m}$. Curve A is the Bowers approximation (4) and (5) for $b = 1$, using $\lambda = \lambda_{\text{eff}}$. Curve B is the "local" solution of Eqs. (9) and (10) also using $\lambda = \lambda_{\text{eff}}$ to include the major effect of nonlocality. Curve D is the nonlocal solution of Eqs. (9) and (12) using $\xi_0 = 3000 \text{ \AA}$ and λ_L , so that the effects of nonlocality due to the restricted mean free path are directly computed from Eq. (11). Curve C is a "pseudolocal" result calculated using the theory of Eqs. (9), (11), and (12) with a small coherence length $\xi_0 = 30 \text{ \AA}$, but compensating by using λ_{eff} in place of λ_L in Eq. (11). Although the Bowers approximation is too strongly peaked, the local, pseudolocal, and nonlocal calculations B–D are really quite comparable, because the principal effect of nonlocality has been inserted via λ_{eff} into the local calculations. The other effect of averaging over a neighborhood is to force the current to half the value it would otherwise have at the very edge of the bridge. However, the rounding induced in the current peak does not greatly affect the maximum value reached.

In Fig. 5 we show the Bowers, pseudolocal, and nonlocal current distributions for the same parameters as Fig. 4, except that the bridge is eight times as wide ($W = 8 \mu\text{m}$). Again there is very little difference between the pseudolocal and nonlocal results C and D. Although the Bowers result A is still too sharply peaked at the edges, it gives a very good account of the current distribution inside the strip for this wider bridge. Although the peak current is important in our critical-current problem, it has very little effect on the magnetic field outside the bridge, and the Bowers approximation has been shown to give adequate agreement with the measurements of such fields by Roderick and Wilson.¹⁸

Using the nonlocal computation, we have computed the enhancement of the peak current $J_{\text{max}}/J_{\text{av}}$ for several widths as a function of λ_L , as shown in Fig. 6. In this case we have assumed $\xi_0 = 2300 \text{ \AA}$ and $\alpha l = d = 1000 \text{ \AA}$. The dashed curves are the results of the Bowers approximation, with $\lambda_{\text{eff}} = 2\lambda_L$ and taking $b = 4$ to reduce the peak density for better agreement. We see that for $Wd \gg \lambda^2$ the computed results approach the results of the Bowers approximation, when b is adjusted to reduce the sharpness of the current peaks.

When the results of Fig. 6 are used to compute $I_c(T)/I_c(0)$, again assuming that $I_c(T)$ occurs when the peak current density reaches J_c^{GL} , we obtain the results of Fig. 7, which are to be compared with Figs. 1 and 2. The theoretical results still show too strong a correction for the nonuniform current flow, apparently overestimating the correction by a factor of 2.

V. NONLINEAR PEAK CURRENT DENSITY

In order to check the validity of the assumption that the critical current is reached when the peak current density reaches J_c^{GL} , we have analyzed a related one-dimensional problem in which the y variations of the vector potential are ignored, which results in an exponential falloff of the currents toward the center of the one-dimensional distribution. Thus, physically, this problem is related to the falloff of the Meissner screening

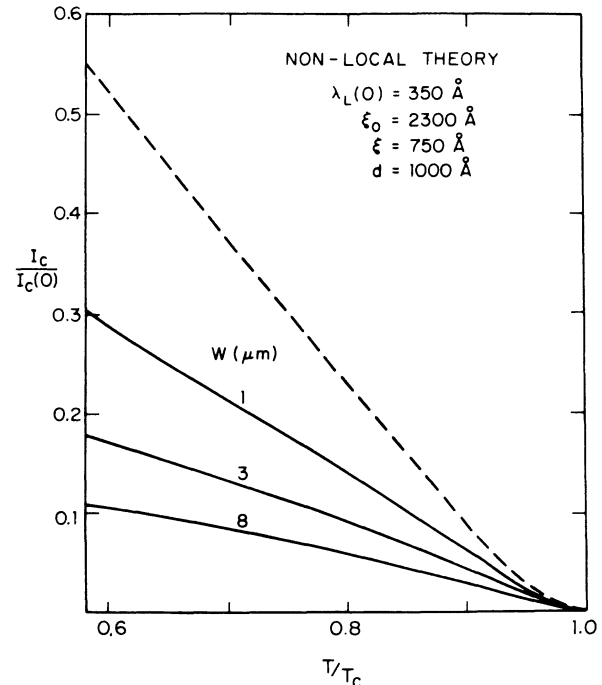


FIG. 7. Theoretical scaled critical currents using nonlocal peak current density and $J_c = J_c^{\text{GL}}$. The dashed curve is the simple GL theory.

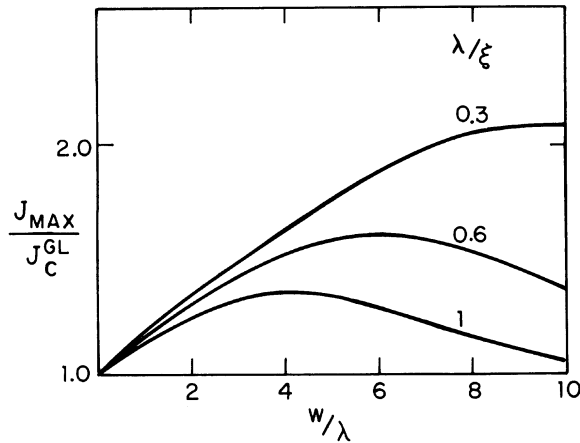


FIG. 8. Enhancement of J_c above J_c^{GL} from the one-dimensional nonlinear GL equations when the coherence length ξ exceeds the penetration depth λ .

currents from the surface of an infinite slab in parallel fields.

In this one-dimensional case the GL equations can be written

$$\lambda^2 \frac{d^2 Q}{dx^2} = f^2 Q = \frac{2}{3\sqrt{3}} \mathcal{G},$$

$$\xi^2 \frac{d^2 f}{dx^2} = f(1 - f^2 - Q^2).$$

Here f is the magnitude of the order parameter normalized to the spatially uniform value in the absence of currents and fields, $\vec{Q} = \nabla\phi - e^* \vec{A}/\hbar c$ is the dimensionless gauge-invariant momentum, \mathcal{G} is J/J_c^{GL} , λ is the penetration depth, and ξ is the GL coherence length. These coupled ordinary differential equations can be solved numerically, assuming symmetry with respect to the center of the bridge and that $df/dx = 0$ at the edge of the bridge. The value of Q at the center of the bridge is related to the total current carried.

These equations describe an exponential variation of the momentum with a characteristic length scale set by the penetration depth, and a depression of the order parameter at large momenta with the spatial variation of the order parameter limited to the scale of the coherence length. If the co-

herence length exceeds the penetration depth, it is possible for peak current densities larger than J_c^{GL} to be achieved, since the magnitude of the order parameter is held up in the region of peak momentum by the coherence-length effect. Figure 8 shows the results of numerical calculations of the magnitude of this enhancement for various dimensions and coherence lengths.

Similar enhancements should be expected in real bridges where the current density peaks at the edge, but does not get exponentially small in the center of the bridge. If the coherence length exceeds the penetration depth, then the full depairing effect should not occur at the sharp peak in the momentum distribution. Since our clean bridges generally have a coherence length at least twice the penetration depth, it is reasonable to assume that the additional factor-of-2 correction needed to account completely for the observed magnitudes of the critical currents of our wide bridges can be attributed to this enhancement of the peak current density above J_c^{GL} .

VI. CONCLUSIONS

We have measured the critical currents of long uniform superconducting microbridges ranging in width from 0.3 to 10 μm . In the narrowest bridges the magnitude and temperature dependence of the critical current density agree with J_c^{GL} . In wider bridges the current density becomes peaked at the edges of the film and the temperature dependence and magnitude of the critical current are altered. We have based our approximate solution of the theoretical problem on separate calculations of the linear electrodynamics assuming nonlocality, and of the nonlinear peak current density assuming spatial variation of the order parameter governed by $\xi(T)$. The primary effect of nonlocality is to introduce λ_{eff} . The linear electrodynamics together with peak current density J_c^{GL} explains the temperature dependence of I_c for the wide bridges, although the correction is approximately a factor of 2 too large. Our nonlinear calculations show that enhancement of the peak current density above J_c^{GL} should be expected when $\xi(T) > \lambda(T)$ and may explain the residual discrepancy.

*Research supported by the National Science Foundation and the Joint Services Electronics Program.

¹V. L. Ginzburg and L. D. Landau, *Zh. Eksp. Teor. Fiz.* **20**, 1064 (1950).

²L. N. Cooper, in *Proceedings of the Seventh International Conference on Low Temperature Physics*, edited by G. M. Graham and A. C. Hollis Hallett (Toronto U. P., Toronto, Canada, 1960), p. 416.

³P. M. Marcus, in *Proceedings of the Seventh Interna-*

tional Conference on Low Temperature Physics, edited by G. M. Graham and A. L. Hollis Hallett (Toronto U. P., Toronto, Canada, 1960), p. 418.

⁴K. K. Likharev, *Radiofizika* **14**, 909 (1971).

⁵K. K. Likharev, *Radiofizika* **14**, 919 (1971).

⁶For a review, see, K. L. Chopra, *Thin Film Phenomena* (McGraw-Hill, New York, 1969), p. 566.

⁷R. E. Glover, III and H. T. Coffey, *Rev. Mod. Phys.* **36**, 299 (1964).

- ⁸T. K. Hunt, *Phys. Rev.* 151, 325 (1966).
- ⁹V. P. Andratskii *et al.*, *Zh. Eksp. Teor. Fiz.* 65, 1591 (1973) [*Sov. Phys.-JETP* 38, 794 (1974)].
- ¹⁰W. J. Skocpol, M. R. Beasley, and M. Tinkham, *J. Low Temp. Phys.* 16, 145 (1974).
- ¹¹W. J. Skocpol, M. R. Beasley and M. Tinkham, *J. Appl. Phys.* 45, 4054 (1974).
- ¹²M. Tinkham, *Introduction to Superconductivity* (McGraw-Hill, New York, 1975), p. 77.
- ¹³R. Meservey and B. B. Schwartz, in *Superconductivity*, edited by R. D. Parks (Marcel Dekker, New York, 1969), p. 167.
- ¹⁴J. Bardeen, L. N. Cooper, and J. R. Schrieffer, *Phys. Rev.* 108, 1175 (1957).
- ¹⁵R. A. Bowers (unpublished), cited in Ref. 18.
- ¹⁶J. Pearl, *J. Appl. Phys.* 37, 2956 (1966).
- ¹⁷A. R. Sass and I. D. Skurnick, *J. Appl. Phys.* 36, 2260 (1965).
- ¹⁸E. H. Roderick and E. M. Wilson, *Nature* 194, 1167 (1962).